Atmos. Chem. Phys. Discuss., https://doi.org/10.5194/acp-2018-356
Manuscript under review for journal Atmos. Chem. Phys.
Discussion started: 16 May 2018

Atmospheric Chemistry and Physics Discussions

Sources and processes that control the submicron organic aerosol in an urban Mediterranean environment (Athens) using high temporal resolution chemical composition measurements.

Iasonas Stavroulas[1,2], Aikaterini Bougiatioti[1,3], Despina Paraskevopoulou[3], Georgios Grivas[3], Eleni Liakakou[3], Evangelos Gerasopoulos[3] and Nikolaos Mihalopoulos[1,3]

[1]Environmental Chemical Processes Laboratory, Department of Chemistry, University of Crete, 71003 Crete, Greece
[2]Energy Environment and Water Research Center, The Cyprus Institute, Nicosia 2121, Cyprus
[3]Institute for Environmental Research and Sustainable Development, National Observatory of Athens, Lofos Koufou, P. Penteli, 15236, Athens, Greece

Correspondence to: A. Bougiatioti (kbougiatioti@gmail.com) and N. Mihalopoulos (nmihalo@noa.gr)

Abstract. Submicron aerosol chemical composition has been studied during a year-long period (26/07/2016-31/07/2017) and two winter-time intensive campaigns (18/12/2013 – 21/02/2014 and 23/12/2015 – 17/02/2016), at a central site in Athens, Greece, using an Aerosol Chemical Speciation Monitor (ACSM). Concurrent measurements include a Particle-Into-Liquid Sampler (PILS-IC), a Scanning Mobility Particle Sizer (SMPS), an AE-33 Aethalometer and Ion Chromatography analysis on 24 or 12 hour filter samples. Quality of the ACSM data was assured by comparison versus the above mentioned measurements. The aim of the study was to characterize the seasonal variability of the main fine aerosol constituents and decipher the sources of organic aerosol (OA). Organics were found to contribute almost half of the submicron mass, with concentrations during wintertime reaching up to 200 μg m^{-3}, on occasions. During this season, the primary sources contribute about 34% of the organic fraction, comprising of biomass burning (10%), fossil fuel combustion (16%) and cooking (8%), while the remaining 66% is attributed to secondary aerosol. The semi-volatile component of the oxidized organic aerosol (SV-OOA; 31%) was found to be clearly linked to combustion sources and in particular biomass burning, and even a part of the very oxidized, low-volatility component (LV-OOA; 35%) could also be attributed to the oxidation of emissions from these primary combustion sources. These results highlight the

Atmos. Chem. Phys. Discuss., https://doi.org/10.5194/acp-2018-356
Manuscript under review for journal Atmos. Chem. Phys.
Discussion started: 16 May 2018

Atmospheric Chemistry and Physics Discussions

rising importance of biomass burning in urban environments during wintertime, as revealed through this characteristic example of Athens, Greece, where the economic recessions led to an abrupt shift to biomass burning for heating purposes in winter. During summer, when concentrations of fine aerosols are considerably lower, more than 80% of the organic fraction is attributed to secondary aerosol (SV-OOA 30% and LV-OOA 53%). In contrast to winter, SV-OOA appears to result from a well-mixed type of aerosol, linked to fast photochemical processes and the oxidation of primary traffic and biogenic emissions. Finally, LV-OOA presents a more regional character in summer, owing to the oxidation, within a few days, of organic aerosol.

1. Introduction

The Greater Athens Area (GAA) has over 4 million inhabitants, gathering more than 40% of the total population of Greece in a basin on the west coast of the Attica Peninsula (450 km^2) (Kanakidou et al., 2011; Grivas et al., 2012). Being surrounded by mountains on three sides, the topography of the area is quite unfavorable to dispersion of air pollutants and ventilation takes place mostly under northeasterly flow (Kanakidou et al., 2011; Grivas et al., 2012; Pateraki et al., 2014). Under low wind speed conditions and the absence of removal via wet deposition, high levels of atmospheric pollutants are observed, significantly deteriorating the air quality of the city (Fourtziou et al., 2017).

The GAA is influenced by long-range transport of atmospheric particulate matter, as well as by significant local sources, namely traffic, industrial activities and combustion of fossil fuel and biomass, the latter especially during wintertime. Particulate matter is considered as the highest priority pollutant to mitigate with respect to population exposure risks, as severe exceedances of the PM_{10} air quality standards and elevated concentrations are frequently encountered, especially during the cold period (Chaloulakou et al., 2005).

The economic recession in Greece, making its trace notable on population during the past decade, has initially caused deceleration of industrial activity and reduction of vehicular circulation (Vrekoussis et al., 2013; Paraskevopoulou et al., 2014). At a later stage, the crisis compelled the residents to switch from fossil fuel combustion for domestic heating to sometimes uncontrolled burning of wood and biomass, leading to significant air quality deterioration of an episodic nature (Saffari et al., 2013, Fourtziou et al., 2017, Gratsea et al., 2017). During winter, wood combustion is one of the major sources of organic aerosol (OA) in Europe (Puxbaum et al., 2007; Kalogridis

et al., 2017) and besides primary particles, that consist of a complex mixture of soot, inorganic and organic matter (OM), a considerable amount of volatile organic compounds (VOCs) are also emitted from wood burning, some of which are known to lead to secondary organic aerosol (SOA) formation (Heringa et al., 2012).

The emissions and properties of the smoke from burning activities can be highly variable, depending significantly on the type of biomass burned (Lathem et al., 2013). The chemical aging of biomass burning (BB) primary organic aerosol (POA) via photochemistry that leads to the formation of oxygenated organic aerosol (OOA) has been observed during both chamber (Jimenez et al., 2009) and field studies (DeCarlo et al., 2010; Cubison et al., 2011). Moreover, it has been recently observed that even within a few hours of atmospheric processing, freshly emitted biomass burning organic aerosol (BBOA) is transformed to more oxidized OA (Lathem et al., 2013; Bougiatioti et al., 2014), and this processing can also take place during night-time, in the absence of sunlight (Bougiatioti et al., 2014). Existing measurements of aerosol chemical composition in Athens have mainly been performed using 24-h filter samples (or 12-h during intensive campaigns) (e.g Theodosi et al., 2011; Paraskevopoulou et al., 2014). Respective measurements using high resolution techniques are scarce and limited in time (Florou et al., 2017).

In this study we present, for the first time, long-term results on the sources of submicron organic aerosols in Athens from high temporal resolution measurements during a year-long period, complemented by two intensive winter campaigns. For the collection of data we deployed an ACSM, a PILS coupled with ion chromatography and auxiliary aerosol and gas phase measurements. The main objectives of this are (i) to characterize the non-refractory part of the submicron aerosol and its variability using high temporal resolution, (ii) to quantify the sources of the organic aerosol and their seasonal variability (via PMF analysis) and (iii) to study the year-to-year changes of aerosol sources during winter time, with special emphasis on wood burning.

2. Experimental Methods

2.1 Sampling site and period

The measurements exploited in this study were conducted, at the urban background site of the National Observatory of Athens at Thissio (37.97N, 23.72E), as representative of the mean population exposure over Athens metropolitan area (Fourtziou et al., 2017). The site stands at an

elevation of 105 m above a moderately populated area, where the influence of direct local emissions is limited.

The measurement period lasted for an entire year, from July 2016 to July 2017. Additionally, two intensive winter campaigns took place at the same site, the first from mid-December 2013 to mid-February 2014 and the second from 23 December 2015 to 17 February 2016. These intensive campaigns aimed at studying the year-to-year variability of biomass burning on the air quality of the city of Athens during wintertime.

2.2 Instruments and Methods

Measurements were performed with an Aerosol Chemical Speciation Monitor (ACSM, s/n 140-139) by Aerodyne Research (Ng et al. 2011a), measuring the non-refractory PM_1 (NR-PM_1) aerosol mass and chemical composition in near real-time (30-minute temporal resolution). The instrument was sampling through a BGI Inc. SCC 1.197 Sharp Cut Cyclone operated at 3 L min^{-1}, yielding a cut off diameter of approximately 2 μm. The ACSM measures mass and provides real time chemical composition (organics, sulfate, nitrate, ammonium and chloride) for non-refractory aerosol particles. The design of the instrument limits these measurements in the submicron range; more specifically the particles that reach the final stage of the instrument lie in the size range from 40 to 700 nm. Practically the ACSM operates following a similar principle as the Aerosol Mass Spectrometer (AMS) (Jayne et al., 2000) where ambient air is drawn through a critical orifice to a particle focusing aerodynamic lens; the resulting particle beam is flash-vaporized at 600ºC, ionized via electron impact ionization and guided through a quadrupole mass spectrometer. The instrument has participated in an intercomparison study of 15 Q-ACSM instruments organized by the European Center for Aerosol Calibration (ECAC) at the Aerosol Chemical Monitor Calibration Center (ACMCC) at Site Instrumental de Recherche par Télédétection Atmosphérique (SIRTA, Paris) during March 2016 (www.actris-ecac.eu/acsm-2016-1.html). It showed excellent agreement (well below ±20%) with the ACMCC's reference instrument, in both pre- and post-calibration periods of the intercomparison study, while the relative ionization efficiencies (RIE) for ammonium and sulfate, obtained by the on-site calibration, were very close to the ones previously used, indicating a stable performance of the instrument. The detection limits for the ACSM provided by Ng et al. (2011a) are: 0.284 μg m^{-3} for ammonium, 0.148 μg m^{-3} for organics, 0.024

μg m^{-3} for sulfate, 0.012 μg m^{-3} for nitrate, and 0.011 μg m^{-3} for chloride. Mass concentrations are calculated with the recommended collection efficiency of 0.5 for all constituents.

Parallel measurements were performed for biomass burning identification, but also for quality control purposes. In this context, a Metrohm ADI 2081 Particle Into Liquid Sampler (Orsini et al., 2003) coupled with Ion Chromatography (Dionex ICS-1500) was used, which was sampling ambient air from a different, but adjacent to the ACSM's, PM_1 inlet. The ion Chromatograph was set to measure cations such as ammonium and potassium at a time resolution of 15 minutes. The resulting concentrations from the ACSM were tested against filter measurements and the concentrations provided by the PILS. For the PILS, the detection limit was calculated at 1 ppb for Na^+, NH_4^+, Mg^{+2} and Ca^{+2} and 2 ppb for K^+. Reported concentrations were blank corrected.

Two different absorption photometers were monitoring Black Carbon (BC) concentrations. A 7-wavelength Magee Scientific AE-42 portable aethalometer was used for the 2013-14 and 2015-16 winter campaigns, providing 5-min resolution measurements. For the year-long period a dual spot, 7-wavelength Magee Scientific AE-33 aethalometer (Drinovec et al., 2015) was used, operating at 1-min resolution. Standard gas analyzers monitoring, like O_3 (Thermo Electron Co., model: 49i), CO, SO_2 and NO_x concentrations (HORIBA, 360 series), a PM_{10} beta-attenuation monitor for aerosol mass concentration (Eberline, FH 62 I-R) and a Scanning Mobility Particle Sizer for PM_1 size distributions (SMPS 3034, TSI Inc.) were also operating at the sampling site, as part of its routine measurements. Wavelength dependent source apportionment of the BC load was performed providing a fossil fuel (BC_{ff}) and a wood combustion (BC_{wb}) generated factor. An absorption exponent of 1 for fossil fuel combustion and 1.9 for pure wood burning based on the approach of Sandradewi et al. (2008) was used, very close to the respective values of 0.9 and 2, used in a suburban site in Athens (Kalogridis et al., 2017). Necessary meteorological parameters for the study were taken from the historic actinometric meteorological station of NOA, at Thissio (Kazadzis et al., 2018). All measurements were averaged to 1-hour intervals in order to synchronize the different data sets.

Four-day back trajectories were calculated using the HYbrid Single-Particle Langrangian Integrated Trajectory (HYSPLIT_4) model (Draxler and Hess, 1998) developed by the ARL/NOAA, and 1-degree GDAS (NCEP) meteorological data. Trajectories were computed every 3-h, for air masses arriving at Athens at a height of 1000 m. The selected height is considered suitable to capture transport at a representative upper limit of the boundary layer in Athens

(Markou and Kassomenos, 2010). Trajectory clustering was performed using the TrajStat plugin (Sirois and Bottenheim, 1995; Wang et al., 2009) of the MeteoInfo GIS software (http://www.meteothinker.com/products/meteoinfo.html). The change of the total space variance for decreasing number of clusters was examined as a criterion for cluster number selection. The analysis was performed separately for summer and winter, resulting in 5 clusters for each period.

2.3 Source apportionment using Positive Matrix Factorization analysis

Positive Matrix Factorization (Paatero and Tapper, 1994) was performed on the organic spectra obtained by the ACSM. The graphic interface SoFi (Source Finder) version 6.1, developed at PSI, Zurich **(**Canonaco et al., 2013) was used. SoFi implements the multilinear engine algorithm ME-2 (Paatero and Hopke, 2003), analyzing the acquired mass spectral timeseries matrix into a linear combination of source profile and time series sub-matrices.

Briefly, the organic mass spectra measured by the ACSM are represented as a matrix X, with columns representing the different m/z's and rows the time series of the mass spectrum. Then the measured matrix X is approximated by the product of F and G, added to E (X=GF+E) where each column of matrix G represents the time series of a factor and each row of F represents the profile (mass spectrum) of this factor and E is the model residual. The entries in F and G are then fitted using a least squares algorithm that iteratively minimizes the quantity Q^m, which is the sum of the squared residuals weighted by their uncertainties. Finally, at each step of the solution process, outliers are defined based on the ratio of residuals to uncertainties (Canonaco et al., 2013).

The input organics and organics' error matrices are derived automatically from the ACSM data analysis software, using a simple automated procedure. Several PMF runs were realized, following the methodology proposed by Crippa et al. (2014). In brief, initially unconstrained runs provided insight on the potential number of factors. For the following steps, primary OA factors were deconvolved by introducing constrains to known factor profiles, implementing the α value approach, while potential secondary oxygenated components were left unconstrained. The α value ranges between 0 and 1 and is a measure of how much the resolved factors are allowed to vary from the input ones. Next, the model's residuals were analyzed in search of structures that could indicate underestimation or overestimation of the number of separated factors. The year-long data series was divided into a cold (November 2016 to March 2017) and warm (August to September 2016 and May to July 2017) period as sources of organics and thus mass spectra and intensities

are expected to differ considerably. A detailed description on the source apportionment method applied can be found in the following section.

3. Results and Discussion

3.1 Comparison of ACSM data with ancillary measurements

As a first quality control/quality assurance of the ACSM data, the ammonium concentrations are compared to the respective ones derived from the PILS, on an hourly basis for winter 2016-17. A very good agreement is found (squared Pearson correlation coefficient R^2=0.83, slope of 0.98). The sulfate and nitrate concentrations for the winter 2016-2017 period are compared to the respective ones from the ion chromatography analysis ($PM_{2.5}$ filters), on a daily basis (R^2=0.69, slope of 0.95 and R^2=0.81, slope of 0.95, respectively). The organics concentrations are compared to the organic carbon concentrations of the $PM_{2.5}$ filters determined by the thermal-optical method (SUNSET Laboratory Inc.) using the EUSAAR-2 protocol (Cavalli et al., 2010). A very good agreement is found (squared Pearson correlation coefficient R^2=0.94, slope of 1.77) with the slope being close to values reported for urban areas (Petit et al., 2015) and OM:OC calculations from AMS measurements in polluted environments (Saarikoski et al., 2012). The results from the aforementioned comparisons are provided in the Supplementary material (SI.1.1).

During the intensive winter 2015-2016 campaign, the concentrations of the ACSM components are compared to those determined from the ion chromatography, based on concurrent filter samples collected at the same site, twice per day, (06:00 - 18:00 pm and t 18:00 - 06:00 local time). Results indicate an excellent agreement for sulfate (R^2=0.88, slope of 0.92), ammonium (R^2=0.81, slope of 1.04), and nitrate (R^2=0.87, slope of 1.08) (Figure SI.1.2). During the intensive winter 2013-2014 campaign, the ammonium concentrations from the ACSM showed significant correlation with the respective ones from the PILS (R^2=0.81, slope of 0.97).

Finally, the sum of the ACSM component concentrations plus BC, measured with the 7-wavelength aethalometer was compared with the mass concentrations determined by a Scanning Mobility Particle Sizer (SMPS; TSI 3034) measuring particle number concentrations in the range of 10.4-469.8 nm (since February 2017 at Thissio). The results obtained using a constant collection efficiency of 0.5, are portrayed in Figure 1 and indicate strong correlation (squared Pearson correlation coefficient R^2=0.88) a slope of 0.90 and an insignificant intercept of 0.01. The slight underestimation of the SMPS-derived submicron mass can be attributed to the instrument's upper

limit diameter (469.8 nm versus 700 nm for the ACSM). It should also be noted that this discrepancy could be attributed to the uncertainty in the estimation of aerosol density used for the conversion of volume to mass concentration of the SMPS (Bougiatioti et al., 2014).

3.2 PM_1 average chemical composition and seasonality

3.2.1 Chemical composition and characteristics

The time series of the main submicron aerosol components measured by the ACSM and the black carbon concentrations are presented in the upper panel of Figure 2 (one complete year period). The average cumulative concentration of the ACSM components and BC was 15.1±16.7 μg m^{-3}. The highest concentrations were measured during winter (average 20.9±26.4 μg m^{-3}) and the lowest during summer (average 9.1.±6.2 μg m^{-3}). On an annual basis, the most abundant component was organic aerosol, followed by sulfate, contributing 46.1 and 29.1% to the total submicron mass, respectively, while BC contribution was calculated at 12%, ammonium 8.5% and nitrate 4.3%. In the middle and bottom panels of Figure 2 the respective time series of the main submicron aerosol components during the two intensive 2-month winter campaigns are presented. During winter 2013-14 the average mass concentration of the ACSM components (plus BC concentrations) was 25.1±29.9 μg m^{-3}, with organics and sulfate contributing 53.5 and 15.9% to the total submicron mass, respectively, followed by BC (12.9%). During winter 2015-16 the average concentration was 19.5±25.3 μg m^{-3}, with organics and BC contributing 51.2 and 17.9% to the total submicron mass, respectively, followed by sulfate (17.6%), nitrate (6.7%) and ammonium (6.6%). It is clearly deduced that during the last winters, organics constitute half or even more of the total PM_1 mass, sulfate around 20% and BC around 14%.

What is also striking is the fact that during wintertime, PM_1 concentration spikes can reach up to 240 μg m^{-3} hourly values, with organics taking up most of the mass. Maxima are recorded during night-time and mostly during meteorological conditions favoring pollutants emission and accumulation, such as low wind speed and low temperature (Fourtziou et al., 2017). There are on average 8 such incidents occurring during each winter (10 in 2013-14, 7 in 2015-16 and 8 in 2016-17), with organic levels being higher than 100 μg m^{-3}. Such levels are the highest reported for Europe during wintertime and highlight the impact of local emissions and especially those related to heating/wood burning (see below), to the levels of organics and consequently PM_1. These observations are in accordance with Florou et al. (2017, same site from 10 January until 9 February

2013), whereas organics concentration alone reached up to 125 μg m^{-3} and maxima of 8 μg m^{-3} for BC and up to 5 μg m^{-3} for nitrate, were recorded. Similarly, wintertime pollution events with increased local character and elevated organics concentrations (around 100 μg m^{-3}, average of 22.6 μg m^{-3}) have been reported at a regional background site, just outside of Paris, during February 2012 (Petit et al., 2015).

3.2.2 Seasonal variability

The seasonal variability of the main measured species, along with the average PM_1 concentration (μg m^{-3}), as calculated from the ACSM+BC measurements is shown in Figure 3 and the basic statistics are included in Table 1. Organics contribute 43.9% to the total submicron aerosol mass in summer, followed by sulfate (33.1%), ammonium (12.5%) and BC (7.6%), while in winter, organics and sulfate contribute 49.1 and 24.1%, respectively, followed by BC (12.1%), ammonium (6.9%) and nitrate (6.7%).

The mass concentrations of organics, nitrate, chloride and BC exhibit a clear annual cycle, with minimum during summer and maximum in winter. This pattern seems to be due to a combination of three simultaneous processes. At first, the additional primary emissions from heating play an important role. A second reason could be the decreased boundary layer depth during winter. According to Kassomenos et al., 1995, daytime PBL depth shows a clear annual cycle, with maxima during the warm months (June to September) and exhibiting a two-fold decrease during wintertime. Finally, the effect of temperature to the partitioning of the semi-volatile inorganics can also contribute to the processes leading to the observed pattern. In support of the above, larger standard deviation is found in winter, demonstrating the frequency and magnitude of the observed pollution events due to the increased need for heating purposes (Fourtziou et al., 2017). Independently of the year, it can be seen that winter concentrations of organics, nitrate, chloride and BC are very similar and more than twice the respective ones during the rest of the seasons (Table 1).

Organics concentration are consistently high during all studied winters (from December to February), while the higher nitrate values can be also attributed to the increased local sources combined with the overall lower temperatures, which favor the stability of ammonium nitrate (Park et al., 2005; Mariani and de Mello, 2007). Ammonium and sulfate exhibit the opposite seasonal cycle, with maximum values in summer and minimum during winter and spring. The higher

summer sulfate levels are the result of enhanced photochemistry associated with more intense insolation, combined with less precipitation, favoring the regional transport of polluted air masses (Cusack et al., 2012). The seasonal variation of concentrations is in agreement with that observed in Athens, during prior long-term measurement campaigns based on analysis of daily filter samples (Theodosi et al. 2011, Paraskevopoulou et al., 2014; 2015).

3.2.3 Diurnal variability

When investigating the diurnal patterns of the measured species (Figure 4), it is observed that during wintertime, ammonium and sulfate do not exhibit any significant variability, which is due to the more regional character of ammonium sulfate (Seinfeld and Pandis, 2016). In order to quantify the extent of this variability we calculated the normalized diurnal pattern by dividing each hourly value with the respective mean concentration. More specifically, sulfate varies by 12.5% around the mean value while ammonium varies by 33%. On the other hand, organics, BC and nitrate vary significantly during the day (83.4%, 79.8% and 74.3% respectively).These species clearly double their concentrations during night-time, caused by the additional primary emissions. Furthermore, BC and nitrate also exhibit a second maximum during early morning hours, which should be attributed to the primary emissions during the morning traffic rush–hour.

During summer, all concentrations are significantly lower, especially organics (note scale change) which exhibit a 5-fold decrease of their mean maximum concentration during night-time. Normalizing the diurnals, as mentioned above, reveals a much less pronounced variability for organics (46.9%), implying a more regional character, while BC and nitrate exhibit the highest variability (67.7% and 57.6% respectively) in accordance to their local nature. The night-time maxima of BC vanishes, nitrate shows much lower concentrations, due to nitrate partitioning between gas and aerosol phase, favoring the vaporization of ammonium nitrate. BC still exhibits only one maximum during early morning hours owing to traffic emissions. Ammonium and sulfate diurnal profile follows expected photochemistry patterns, with peaking concentrations around 14:00 LT (UTC+2), consistent with secondary aerosol formation and increased vertical mixing with regional aerosol from aloft due to the evolution of the convective boundary layer which exhibits a bell shaped diurnal structure ranging from a few hundred meters to above one kilometer, with maximum heights during early afternoon (Asimakopoulos et al., 2004; Tombrou et al., 2007). Sulfate concentrations exhibit lower night-time background, a concurrent (to winter) primary

Atmos. Chem. Phys. Discuss., https://doi.org/10.5194/acp-2018-356
Manuscript under review for journal Atmos. Chem. Phys.
Discussion started: 16 May 2018

maximum (8:00-10:00 LT), and a secondary significant increase later in the afternoon (twice the night-time background). Finally, organics concentrations are somewhat higher during early night which could possibly be associated with biogenic/vegetation sources either local or regional that produce volatile compounds and condense on the particulate phase during night when temperatures are lower. Furthermore organic variation also follows the morning peak related to traffic and the late afternoon peak also observed for ammonium and sulfate. Condensation of the particulate phase could also apply for nitrate, which also exhibits higher concentrations during night-time (almost double).

3.3 Source apportionment of organic aerosol

A source apportionment analysis of the organic aerosol data was carried out, separately for the cold (1 November to 31 March) and the warm period (July-August-September 2016 and May-July 2017). The separation served to better characterize the different profiles of the sources, as it is expected that the different m/z intensities vary throughout the year. Several runs were performed, following the technical guidelines and methodology proposed by Crippa et al. (2014). Initially, an unconstrained run with the number of factors ranging from 2 to 8 was performed, allowing for a first estimate of the number of potential deconvolved primary and secondary OA spectra. After identifying the presence of primary OA, namely hydrocarbon-like organic aerosol (HOA), cooking organic aerosol (COA) for both periods and BBOA for the winter period, several constrained runs were performed using the α value approach.

In this context, the HOA mass spectrum was first constrained with a low α value, ranging from 0.05 to 0.1, using as reference the average HOA mass spectrum from Ng et al. (2011b). COA was also constrained with an α value ranging from 0.1 to 0.2, using as reference the mass spectrum from Crippa et al. (2013) reported for Paris. Finally, for the three wintertime periods, BBOA was also constrained with higher α values, (between 0.3 and 0.5) using as reference the average BBOA mass spectrum from Ng et al. (2011b). Only $m/z \leq 120$ were used in order to avoid interferences from the naphthalene signal (m/z 127, 128 and 129). Weak signals, with signal-to-noise ratio (S/N) below 0.2 were downweighted by a factor of 10, and those with S/N between 0.2 and 1 were downweighted by a factor of 2 (Ulbrich et al., 2009), using the aforementioned customized software. Solutions were chosen based on specific indicators, such as the Q/Q_{exp} ratio, residual analysis, reproducibility of factors for different model seeds, the affinity of the deconvolved

spectra with spectra found in the AMS mass spectral database (http://cires.colorado.edu/jimenez-group/AMSsd/) and also the correlation of the time series with external time series (such as BC, NO, CO and nss-K^+). The profiles of all solutions were inter-compared as means for sensitivity analysis and the results are provided in the Supplementary material (SI.2). The affinity between spectra is expressed using the θ angle approach (Kostenidou et al., 2009). In this context each deconvolved mass spectrum represents a vector. The cosine of the θ angle between two such vectors (e.g. MS_a and MS_b) is equal to the correlation coefficient R between them. The θ angle is calculated using the dot product formula:

$$\theta = cos^{-1}\left(\frac{MS_a MS_b}{|MS_a||MS_b|}\right)$$

Calculated angles less than 15° correspond to $R > 0.96$ thus indicate spectra which are similar to each other, angles between 15° and 30° correspond to $0.96 > R > 0.86$ and indicate some similarity but also some important differences between the compared spectra, while angles larger than 30° correspond to correlation coefficient $R < 0.86$ and thus are considered to indicate spectra that do not compare well.

Warm period: In this period, the selected solution is a two factor constrained run (HOA using α =0.05 and COA using α =0.1) and consists of four factors: HOA (hydrocarbon-like OA), COA-like (cooking-like OA,), SV-OOA (semi-volatile oxygenated OA) and LV-OOA (low-volatility oxygenated OA). The two summer periods have also been treated separately, but the derived spectra were almost identical (θ angles between 1.6 and 11.9 for all derived factors, see SI). The time series of the four identified sources during summer 2017 is shown in Figure 5 along with their diurnal variability and the respective average daily contribution. The mass spectra of the selected solution are also provided in the supplementary material. No primary biomass burning aerosol could be identified, which is justified by the absence of fresh emissions over the city center during the warm period. In the summer periods HOA makes up 5.5% of the total organic fraction, COA around 12% on average (10.9 and 13% for 2016 and 17, respectively). In summer 2016 SV-OOA made up 30.5% and the rest 53% is LV-OOA. In summer 2017, SV-OOA contributes 46% to the total organic fraction while LV-OOA 35%. The dominance of secondary influence (SV-OOA & LV-OOA) is apparent, and accounts for the majority of the organic aerosol. This finding is in accordance with Kostenidou et al. (2015), who reported that 65% of the sampled aerosol during summer can attributed to SOA (SV-OOA & LV-OOA), at a suburban site in Athens.

Atmos. Chem. Phys. Discuss., https://doi.org/10.5194/acp-2018-356
Manuscript under review for journal Atmos. Chem. Phys.
Discussion started: 16 May 2018

Atmospheric Chemistry and Physics Discussions

Since a strong constraint was used for COA (α =0.1), the derived COA mass spectrum is almost identical to the mass spectrum of wintertime COA in Paris (Crippa et al., 2013) with which the constraint was made, having a θ angle of 7º. COA also shares many similarities with the mass spectrum of fresh organic aerosol emissions from meat charbroiling (Kaltsonoudis et al., 2017) (θ=14.5º). When calculating the O:C ratio in COA following the study of Canagaratna et al. (2015) we find a ratio of 0.19, which is comparable to the value of 0.24 obtained for COA during summer at a suburban site in Athens (Kostenidou et al., 2015). Similarly, due to the constraint (α =0.05) HOA is identical (θ=2.5º) with the average HOA spectrum (Ng. et al., 2011b), obtained by averaging together different HOA mass spectra, but is also very similar to HOA reported by Crippa et al. (2014) (θ=4.5º) and HOA from Paris (θ=6.5º) (Crippa et al., 2013). SV-OOA is similar to the SV-OOA reported by Crippa et al. (2014) (θ=14º), and also has many similarities with the average SV-OOA (θ=16.5º) (Ng et al., 2011b) as well as with the laboratory-generated SOA from isoprene via the reactive uptake of epoxydiols (IEPOX) (θ=16.2º) (Budisulistiorini et al., 2013). This type of aerosol is the oxidation product of isoprene, denoting a possible link of SV-OOA with biogenic aerosol. This association is further strengthened by considering its similarities with SOA from biogenic precursors, such as a- and b-pinene (θ=20º and 18º, respectively) (Bahreini et al., 2005), which are maximum during night similarly to SV-OOA. On the other hand, the derived SV-OOA shares some similarities with SOA from diesel exhaust after 4 h of photochemical ageing (Sage et al. 2008). Finally, SV-OOA does not compare well with the mass spectrum from aged organic aerosol emissions from meat charbroiling (Kaltsonoudis et al., 2017) (32º<θ<37º). This indicates that during summer, it is not linked to the oxidation of primary COA, but rather to SOA formation from the oxidation of VOCs from both biogenic and traffic sources. Finally, LV-OOA is identical (θ=3.6º) with the very oxidized regional OOA found in the area (Finokalia, Crete) (Bougiatioti et al., 2014) and has many similarities with the LV-OOA reported by Crippa et al. (2014) (θ=11.7º) and with the average LV-OOA (θ=18.2º) (Ng et al., 2011b). When calculating the elemental ratios based on the study of Canagaratna et al. (2015), the O:C ratio for LV-OOA is 1.2, which is identical to the value of OOA obtained at Finokalia (Bougiatioti et al. 2014).

HOA correlates significantly with nitrate (R^2=0.63) as well as with BC (R^2=0.52) while COA shows moderate correlation with CO (R^2=0.32) and nitrate (R^2=0.36). SV-OOA is highly correlated with nitrate (R^2=0.89), implying common mechanisms in their variability, possibly linked with the partitioning between the gas and particulate phases. The moderate correlation with

CO (R^2=0.39) and BC (R^2=0.39) implies that SV-OOA may, to some extent, partially originate from a combustion source. LV-OOA shows moderate correlation with sulfate (R^2=0.47) and ammonium (R^2=0.44), consistent with the regional character of this factor. Results from the trajectory cluster analysis (Figure 8) show that enhanced LV-OOA levels are related to air masses originating from Eastern Europe and the Black Sea region, which have both been identified as the main areas of influence for secondary aerosols that are regionally processed and transported to Athens (Gerasopoulos et al., 2011; Grivas et al., 2018).

Primary fossil fuel emissions (HOA) are very low during summer, as in July and August most of the Athenians leave for their summer vacations, thus reducing local traffic. Concentrations peak around 7:00 and after 19:00 LT that corresponds to the early morning and evening rush hours in downtown Athens. COA exhibits a slight hump during lunch hours (12-15:00 LT), also seen in the relative contribution of the factor, while a large night-time peak is present at around 22:00 LT. This late peak is consistent with the late dinner hours and operation of tavernas (typical restaurants) in Athens during the touristic season. SV-OOA exhibits two-fold higher concentrations during night-time, which apart from boundary layer dynamics may also be attributed to the condensation of semi-volatile compounds, as also implied by the excellent correlation of SV-OOA with nitrates. Finally, LV-OOA exhibits a peak during mid-day, consistent with increased photochemical processes that lead to further organic aerosol oxidation. In coincidence to that a moderate hump is also observed for SV-OOA.

In summary, during the warm period, the vast majority (more than 80%) of organic aerosol in the area is linked to secondary organic aerosol formation. The semi-volatile product is of mixed origin, linked to quick atmospheric processes, within a few hours, such as photochemistry of primary sources, like biogenic emissions from vegetation, traffic emissions, or to a lesser extent regional biomass burning. On the contrary, the low-volatility product is the result of more extensive oxidation of organic aerosol in the area, within a few days, and has, thus, a more regional character.

Cold period: In this period, the selected solution is a three factor constrained run (HOA using α =0.1, COA using α =0.2, BBOA using α =0.4) and consists of five factors: BBOA (biomass burning OA), HOA, COA, SV-OOA and LV-OOA. The HOA spectra are identical for all studied winter periods ($1.2^o<\theta<5.2^o$) and so are the COA ($3.3^o<\theta<3.9^o$) and LV-OOA spectra ($3.2^o<\theta<3.6^o$). BBOA spectra still have many similarities between them ($9.7^o<\theta<13.3^o$) while SV-

Atmos. Chem. Phys. Discuss., https://doi.org/10.5194/acp-2018-356
Manuscript under review for journal Atmos. Chem. Phys.
Discussion started: 16 May 2018

OOA also exhibit similarities ($12.9^o<\theta<17.1^o$). Indicatively, the solution for winter 2016-17 is presented (Fig. 6), while the respective solutions for winter 2013-14 and 2015-16 are provided in the supplementary material (Fig. SI.2.3). The time series of the five PMF factors for winter 2016-17 are shown in Figure 6 along with their diurnal variability and the hourly contribution of each factor.

HOA during wintertime 2016-17, is almost identical to the average HOA spectrum (Ng. et al., 2011b), as expected due to the constraint, having a θ angle of 5.1^o, HOA from Crippa et al. 2014 ($\theta=5^o$) and HOA from Paris during winter (Crippa et al., 2013) ($\theta=5.8^o$) and from Hyytiälä (Äijälä et al., 2017) ($\theta=9.6^o$). COA is also almost identical to COA from Paris during winter (Crippa et al., 2013) having a θ angle of 6.2^o. It is also very similar to fresh organic aerosol emissions from meat charbroiling (Kaltsonoudis et al., 2017) ($\theta=13.2^o$) and it shares similarities with COA from Hyytiälä (Äijälä et al., 2017) ($\theta=16.9^o$). When calculating the elemental ratios based on the study of Canagaratna et al. (2015) the O:C ratio for COA is 0.18, which is in accordance with the value of 0.11 derived for COA at the same site by Florou et al. (2017). BBOA is very similar to the average BBOA spectrum (Ng. et al., 2011b) having a θ angle of 11.5^o, sharing similarities with biomass burning aerosol from oak ($\theta=15.7^o$), spruce ($\theta=19.8^o$) (Schneider et al. 2006), BBOA from Crippa et al. (2014) ($\theta=20^o$) and with BBOA during wintertime in Zurich (Lanz et al., 2008) ($\theta=23.4^o$). Once more, the calculated O:C ratio for BBOA is 0.25, which is in accordance with the value of 0.27 derived for BBOA at the same site by Florou et al. (2017). SV-OOA spectrum shares similarities with the average SV-OOA from Ng et al. (2011b) ($\theta=21.3^o$), as well as with the IEPOX-OA from Budisulistiorini et al. (2013) ($\theta=22.8^o$), as isoprene main oxidation products such as methyl vinyl ketone and methacrolein are often used as biomass burning tracers (Santos et al., 2017). Similar correlation is also found with IEPOX-OA and SV-OOA during the winter 2015-16 campaign (Supplementary material, SI.2). It shares some similarities with SV-OOA from wintertime in Paris (Crippa et al., 2013) ($\theta=25.2^o$) and SV-OOA from Hyytiälä (Äijälä et al., 2017) ($\theta=26.2^o$). Finally, LV-OOA is almost identical ($\theta=8.3^o$) with the LV-OOA from Crippa et al. (2014), the average LV-OOA from Ng et al. (2011b) ($\theta=8.4^o$), LV-OOA from Zurich during winter (Lanz et al., 2008; $\theta=9.3^o$) while it also shares many similarities ($\theta=15.1^o$) with the oxidized OOA found in the extended area (Finokalia Crete) (Bougiatioti et al., 2014).

Since the identification of BBOA is mainly based on the two fragments of m/z 60 and 73, considered as the "fingerprint" fragments of levoglucosan and biomass burning tracers, BBOA

exhibits indeed excellent correlation with these two fragments (R^2=0.94 and 0.9, respectively). Nss-K^+ is also proposed as a very good tracer for biomass burning and as is reported by Fourtziou et al. (2017), it shows a significant correlation with BC coming from wood burning (BC_{wb}), during wintertime in Athens. Consequently, the time series of nss-K^+ provided by PILS-IC and m/z 60 are studied together. It appears that during both winters (2013-14 and 2016-17) for which nss-K^+ data is available, m/z 60 is in very good agreement with nss-K^+ (R^2=0.85) (Figure 7a). Furthermore BBOA correlates well with BC_{wb} (R^2=0.78), nss-K^+ (R^2=0.62) and with CO (R^2=0.52). SV-OOA correlates significantly with both wood burning "fingerprint" fragments of m/z 60 and 73 (R^2=0.99 for both), BC_{wb} (R^2=0.82), CO (R^2=0.61) (Figure 7b) and nss-K^+ (R^2=0.61), demonstrating the direct link between SV-OOA and primary combustion sources (mainly biomass burning). It can be seen in Figure 8, that increased concentrations of both BBOA and SV-OOA are linked to air masses originating from Northern and Eastern Europe. During wintertime, these flow categories are associated with the prevalence of synoptic-scale northern winds and a decline in temperature in the area, leading to the appearance of PM episodes due to local combustion for residential heating (Paschalidou et al., 2015).

HOA correlates very well with BC (R^2=0.53), CO (R^2=0.54) and with NO (R^2=0.55). COA correlates moderately with nss-K^+ (R^2=0.32) and chloride (R^2=0.27) while low correlation with BC and CO (both R^2=0.22) has also been previously reported at the same site (Florou et al., 2017). Finally, LV-OOA showed a good correlation with ammonium (R^2=0.62), nitrate (R^2=0.63), nss-K^+ (R^2=0.52) and m/z 73 (R^2=0.51), demonstrating that part of the very oxidized OA during wintertime may also originate from combustion sources as well.

Therefore, during the cold period, the organic aerosol in the area linked to secondary organic aerosol formation contributes around 65% to the total organic fraction. In contrast to summer, the semi-volatile product has a very clear origin, linked to the fast oxidation of primary combustion sources (BBOA and HOA), which is also reflected on its diurnal variability as will be discussed shortly (Fig. 6). Its affinity to biomass burning tracers points out that the largest part of it originates from the fast oxidation of BBOA. The low-volatility product is in this case of more local than long-range transport nature, as also highlighted by the almost two-fold higher values during night-time.

The diurnal cycles of the five factors are shown in Figure 6 (bottom left panel). HOA, originating from fossil fuel combustion, exhibits maximum values during night, associated with

combustion from central heating, and presets a secondary peak during early morning traffic rush hour. COA has similar winter and summer diurnal profiles t with a moderate hump during lunch hours (12-15:00 LT) and a large night-time peak (approx. 22:00 LT), controlled by the decrease of the planetary boundary layer. BBOA is characterized by a pronounced diurnal cycle with peaking values during night-time, associated with the production of this component in the evening by combustion for heating purposes. SV-OOA exhibits the largest diurnal amplitude, with night-time values being almost 6-fold higher compared to daytime. A moderate peak during the morning traffic rush hour (partly masked by the high night values), demonstrates its provenance from the oxidation of freshly-emitted primary combustion organic aerosol (both BBOA and HOA). Finally, LV-OOA also exhibits 2-fold higher values during night compared to daytime. It has a secondary peak during the morning traffic rush hour, showing once more that part of the low volatility OA may also originate from the fast oxidation of primary combustion source, as also implied by its correlation with combustion tracers.

Table 2 sums up the contribution of each one of the 5 identified factors during the three studied winters. Overall, during wintertime BBOA constitutes around 10% of the total organic fraction. Based on the diurnal variability of this factor, its contribution is more pronounced during night-time, when concentrations are 4-fold or higher than the daytime ones, matching emissions from fossil fuel combustion (HOA; traffic plus heating). Taking into account that a large part of the semi-volatile OOA (SV-OOA) comes from the rapid oxidation of freshly emitted BBOA, justified via the excellent correlations with biomass burning tracers, the overall contribution of biomass burning becomes even more significant. Given that SV-OOA contributes around 30% to the organic mass, it is evident that during wintertime, biomass burning may contribute almost half of the total organic aerosol, with this contribution maximizing during night-time. More specifically, for BBOA the lowest contribution during daytime is 2.6% reaching a maximum of 19.4% during night (Figure 6, bottom right panel). The same applies to SV-OOA with daytime minimum contribution of 13.5% and night-time maximum of 35.7%. What is also very important is the fact that even though the winter and summer mass spectra of SV-OOA have some similarities (R^2=0.85, θ=21.4°), there are also differences, especially in the origin of this component, as during winter the majority is linked to the oxidation of primary combustion sources, while during summer the absence of a significant correlation with BC or nss-K^+ implies the presence of different sources, both anthropogenic (but not biomass burning) and possibly biogenic.

Atmos. Chem. Phys. Discuss., https://doi.org/10.5194/acp-2018-356
Manuscript under review for journal Atmos. Chem. Phys.
Discussion started: 16 May 2018

4. Summary and conclusions

High temporal-resolution measurements were conducted for an entire year (plus two, two-month duration, intensive measurement campaigns during wintertime) at an urban background site in Athens, using an ACSM, a PILS-IC system and an aethalometer, in excess to routine pollution measurements. During the 16 month measurement period, several pollution events with PM_1 concentrations reaching as high as 240 μg m^{-3} were recorded, all encountered during wintertime nights. In these cases, organics contributed the largest fraction to the submicron particulate mass, with overall contribution during wintertime reaching 50%, followed by sulfate (~20%) and BC (~14%). Within a typical winter day, organics, BC and nitrate double their concentrations during night-time, as a result of the additional primary combustion emissions for heating purposes. During summer, all concentrations are significantly lower, and organics are once more the main aerosol constituent contributing by 44%, followed by sulfate (33%), ammonium (13%) and BC (8%). Within a typical summer day, ammonium and sulfate concentrations peak at about 14:00 LT (UTC+2), consistent with secondary aerosol formation.

Organics, nitrate, chloride and BC exhibited a clear seasonal cycle with maximum during winter and minimum during summer. Sulfate and ammonium exhibited the opposite cycle, as a result of enhanced photochemistry, limited precipitation and higher regional transport.

Based on the source apportionment of the organic aerosol, four factors were identified during summer, namely hydrocarbon-like OA (HOA), cooking-like OA (COA), semi-volatile oxygenated OA (SV-OOA) and low-volatility OA (LV-OOA), and five factors during winter, the same as in summer with the addition of primary biomass burning emissions (BBOA). During summer, HOA makes up 5.7% of the total organic fraction, COA around 12%, and the rest is linked to secondary organics (SV-OOA and LV-OOA). HOA has peaking values during the morning traffic rush hour, and COA mainly during night-time. SV-OOA exhibits two-fold higher concentrations during night-time while LV-OOA exhibits a peak during mid-day, consistent with photochemical processes. The semi-volatile product is clearly of mixed origin, linked to quick atmospheric processing within a few hours, of VOCs emitted from primary sources like vegetation, traffic and to some limited extent to processed regional biomass burning. The low-volatility product, on the other hand, is the result of more excessive oxidation, in the order of several days, having thus a more regional character.

555 Combining the results from the three different winter campaigns, HOA accounts for almost 16% of the organic fraction, COA around 8%, BBOA 10%, SV-OOA 31% and LV-OOA 35%. All constituents exhibit significantly higher concentrations during night-time, with HOA being affected by combustion from central heating and presenting a secondary peak during the morning traffic rush hour. COA has a similar diurnal profile to the one observed during summer. BBOA is 560 also characterized by a pronounced diurnal cycle with peaking values during night from combustion for heating purposes. SV-OOA has almost 6-fold higher concentrations during night, consistent with its link to the oxidation of primary combustion sources, while even LV-OOA exhibits almost 2-fold higher concentrations during night. In contrast to summer, the semi-volatile product during winter has a very clear origin, linked to the fast oxidation of primary combustion 565 sources (HOA and BBOA) with BBOA being the major source, due to the affinity of SV-OOA with biomass burning tracers. Part of the LV-OOA, as well, could originate from the extensive oxidation of the local primary combustion sources, showing that LV-OOA during winter is of more local than regional character.

Concluding, it is clear that organic aerosol constitutes a large fraction of submicron aerosol 570 throughout the year, in the urban environment of Athens. During wintertime, a large part of this OA, as high as 50%, originates from combustion sources for heating purposes, such as central heating and biomass burning, causing significant air quality deterioration. Night-time contribution of BBOA is 7-fold higher than the one during day, while the respective contribution of SV-OOA is increased by a factor of 2.6. Given that during wintertime, fine PM concentrations reach up to 575 240 μg m^{-3}, the significance of these sources contribution becomes even more striking, demonstrating the necessity for strategic, long-term mitigation actions.

Acknowledgments

580 I. Stavroulas and N. Mihalopoulos acknowledge support by the State Scholarship Foundation ("IKY Fellowships of Excellence for Postgraduate Studies in Greece -Siemens Programme, 2016-2017"), in the framework of the Hellenic Republic-Siemens Settlement Agreement. The authors would also like to acknowledge support from Francesco Canonaco and Andre Prévôt from PSI, who developed SoFi and provided valuable input related to Positive Matrix Factorization. This 585 study contributes to ChArMEx work package 1 on emissions and sources.

References

Äijälä, M., Heikkinen, L., Fröhlich, R., Canonaco, F., Prévôt, A. S. H., Junninen, H., Petäjä, T., Kulmala, M., Worsnop, D., and Ehn, M.: Resolving anthropogenic aerosol pollution types – deconvolution and exploratory classification of pollution events, Atmos. Chem. Phys., 17, 3165-3197, doi:10.5194/acp-17-3165-2017, 2017.

Asimakopoulos, D.N., Helmis, C.G. and Michopoulos, J.: Evaluation of SODAR methods for the determination of the atmospheric boundary layer mixing height, Meteorology and Atmospheric Physics, 85(1-3), 85-92, doi:10.1007/s00703-003-0036-9, 2004.

Bahreini, R., Keywood, M.D., Ng, N.L., Varutbangkul, V., Gao, S., Flagan, R.C., Seinfeld, J.H., Worsnop, D.R. and Jimenez, J.L. Measurements of secondary organic aerosol from oxidation of cycloalkenes, terpenes, and m-xylene using an Aerodyne aerosol mass spectrometer, Environmental science & technology, 39(15), 5674-5688., doi:10.1021/es048061a, 2005

Bougiatioti, A., Stavroulas, I., Kostenidou, E., Zarmpas, P., Theodosi, C., Kouvarakis, G., Canonaco, F., Prevot, A.S.H., Nenes, A., Pandis, S.N., Mihalopoulos, N.: Processing of biomass-burning aerosol in the eastern Mediterranean during summertime, Atmos. Chem. Phys. 14 (9), 4793-4807, doi:10.5194/acp-14-4793-2014, 2014.

Budisulistiorini, S.H., Canagaratna, M.R., Croteau, P.L., Marth, W.J., Baumann, K., Edgerton, E.S., Shaw, S.L., Knipping, E.M., Worsnop, D.R., Jayne, J.T., Gold, A., and Surratt, J.D.: Real-time continuous characterization of secondary organic aerosol derived from isoprene epoxydiols in downtown Atlanta, Georgia using the Aerodyne Aerosol Chemical Speciation Monitor, Environ. Sci. Technol., 47 (11), 5686-5694, doi:10.1021/es400023n, 2013.

Canagaratna, M. R., Jimenez, J. L., Kroll, J. H., Chen, Q., Kessler, S. H., Massoli, P., Hildebrandt Ruiz, L., Fortner, E., Williams, L. R., Wilson, K. R., Surratt, J. D., Donahue, N. M., Jayne, J. T., and Worsnop, D. R.: Elemental ratio measurements of organic compounds using aerosol mass spectrometry: characterization, improved calibration, and implications, Atmos. Chem. Phys., 15, 253-272, doi:10.5194/acp-15-253-2015, 2015.

Canonaco, F., Crippa, M., Slowik, J. G., Baltensperger, U., and Prévôt, A. S. H.: SoFi, an IGOR-based interface for the efficient use of the generalized multilinear engine (ME-2) for the source apportionment: ME-2 application to aerosol mass spectrometer data, Atmos. Meas. Tech., 6, 3649-3661, doi:10.5194/amt-6-3649-2013, 2013.

Cavalli F., Viana M., Yttri K.E., Genberg J., Putaud J.P.: Toward a standardised thermal–optical protocol for measuring atmospheric organic and elemental carbon: The EUSAAR protocol, Atmos. Meas. Techniques, 3, 79-89, doi:10.5194/amt-3-79-2010, 2010.

Chaloulakou, A., Kassomenos, P., Grivas, G., and Spyrellis, N.: Particulate matter and black smoke concentration levels in central Athens, Greece, Environ. Int., 31, 651-659, doi:10.1016/j.envint.2004.11.001, 2005.

Crippa, M., DeCarlo, P. F., Slowik, J. G., Mohr, C., Heringa, M. F., Chirico, R., Poulain, L., Freutel, F., Sciare, J., Cozic, J., Di Marco, C. F., Elsasser, M., Nicolas, J. B., Marchand, N., Abidi, E., Wiedensohler, A., Drewnick, F., Schneider, J., Borrmann, S., Nemitz, E., Zimmermann, R., Jaffrezo, J.-L., Prévôt, A. S. H., and Baltensperger, U.: Wintertime aerosol chemical composition and source apportionment of the organic fraction in the metropolitan area of Paris, Atmos. Chem. Phys., 13, 961-981, doi: 10.5194/acp-13-961-2013, 2013.

Crippa, M., Canonaco, F., Lanz, V. A., Äijälä, M., Allan, J. D., Carbone, S., Capes, G., Ceburnis, D., Dall'Osto, M., Day, D. A., DeCarlo, P. F., Ehn, M., Eriksson, A., Freney, E., Hildebrandt Ruiz, L., Hillamo, R., Jimenez, J. L., Junninen, H., Kiendler-Scharr, A., Kortelainen, A.-M., Kulmala, M., Laaksonen, A., Mensah, A. A., Mohr, C., Nemitz, E., O'Dowd, C., Ovadnevaite, J., Pandis, S. N., Petäjä, T., Poulain, L., Saarikoski, S., Sellegri, K., Swietlicki, E., Tiitta, P., Worsnop, D. R., Baltensperger, U., and Prévôt, A. S. H.: Organic aerosol components derived from 25 AMS data sets across Europe using a consistent ME-2 based source apportionment approach, Atmos. Chem. Phys., 14, 6159-6176, doi:10.5194/acp-14-6159-2014, 2014.

Cubison, M. J., Ortega, A. M., Hayes, P. L., Farmer, D. K., Day, D., Lechner, M. J., Brune, W. H., Apel, E., Diskin, G. S., Fisher, J. A., Fuelberg, H. E., Hecobian, A., Knapp, D. J., Mikoviny, T., Riemer, D., Sachse, G. W., Sessions, W., Weber, R. J., Weinheimer, A. J., Wisthaler, A., and Jimenez, J. L.: Effects of aging on organic aerosol from open biomass burning smoke in aircraft and laboratory studies, Atmos. Chem. Phys., 11, 12049–12064, doi:10.5194/acp-11-12049-2011, 2011.

Cusack M, Alastuey A, Pérez N, Pey J, Querol X.: Trends of particulate matter ($PM_{2.5}$) and chemical composition at a regional background site in the Western Mediterranean over the last nine years (2002-2010), Atmos. Chem. Phys., 12, 8341–8357, doi:10.5194/acp-12-8341-2012, 2012.

DeCarlo, P. F., Ulbrich, I. M., Crounse, J., de Foy, B., Dunlea, E. J., Aiken, A. C., Knapp, D., Weinheimer, A. J., Campos, T., Wennberg, P. O., and Jimenez, J. L.: Investigation of the sources and processing of organic aerosol over the Central Mexican Plateau from aircraft measurements during MILAGRO, Atmos. Chem. Phys., 10, 5257–5280, doi: 10.5194/acp-10-5257- 2010, 2010.

Draxler, R.R. and Hess, G.D.: An overview of the HYSPLIT_4 modelling system for trajectories, dispersion, and deposition, Austr. Meteor. Mag., 47, 295-308, 1998.

Drinovec, L., Močnik, G., Zotter, P., Prévôt, A. S. H., Ruckstuhl, C., Coz, E., Rupakheti, M., Sciare, J., Müller, T., Wiedensohler, A., and Hansen, A. D. A.: The "dual-spot" Aethalometer: an improved measurement of aerosol black carbon with real-time loading compensation, Atmos. Meas. Tech., 8, 1965-1979, doi: 10.5194/amt-8-1965-2015, 2015.

Florou, K., Papanastasiou, D. K., Pikridas, M., Kaltsonoudis, C., Louvaris, E., Gkatzelis, G. I., Patoulias, D., Mihalopoulos, N., and Pandis, S. N.: The contribution of wood burning and other pollution sources to wintertime organic aerosol levels in two Greek cities, Atmos. Chem. Phys., 17, 3145-3163, doi: 10.5194/acp-17-3145-2017, 2017.

Fourtziou, L., Liakakou, E., Stavroulas, I., Theodosi, C., Zarmpas, P., Psiloglou, B., Sciare, J., Maggos, T., Bairachtari, K., Bougiatioti, A. and Gerasopoulos, E.: Multi-tracer approach to characterize domestic wood burning in Athens (Greece) during wintertime. Atmospheric Environment, 148, 89-101, doi:10.1016/j.atmosenv.2016.10.011, 2017.

Gerasopoulos, E., Amiridis, V., Kazadzis, S., Kokkalis, P., Eleftheratos, K., Andreae, M.O., Andreae, T.W., El-Askary, H., Zerefos, C.S.: Three-year ground based measurements of aerosol optical depth over the Eastern Mediterranean: The urban environment of Athens, Atmos. Chem. Phys. 11, 2145-2159, doi:10.5194/acp-11-2145-2011 2011.

Gratsea, M., Liakakou, E., Mihalopoulos, N., Adamopoulos, A., Tsilibari, E., and Gerasopoulos, E.: The combined effect of reduced fossil fuel consumption and increasing biomass combustion on Athens' air quality, as inferred from long term CO measurements, Sci. Tot. Environ., 592, 115-123, doi:10.1016/j.scitotenv.2017.03.045, 2017.

Grivas, G., Cheristanidis, S., and Chaloulakou, A.: Elemental and organic carbon in the urban environment of Athens. Seasonal and diurnal variations and estimates of secondary organic carbon, Sci. Tot. Environ., 414, 535-545, doi:10.1016/j.scitotenv.2011.10.058, 2012.

Grivas, G., Cheristanidis, S., Chaloulakou, A., Koutrakis, P., Mihalopoulos, N.: Elemental composition and source apportionment of fine and coarse particles at traffic and urban background locations in Athens, Greece. Aerosol and Air Quality Research, in press, doi: 10.4209/aaqr.2017.12.0567, 2018.

Heringa, M.F., DeCarlo, P.F., Chirico, R., Lauber, A., Doberer, A., Good, J., Nussbaumer, T., Keller, A., Burtscher, H., Richard, A., Miljevic, B., Prevot, A.S.H., Baltensperger, U.: Time-Resolved characterization of primary emissions from residential wood combustion appliances, Environ. Sci. Technol. 46, 11418-11425, doi:10.1021/es301654w, 2012.

Jayne, J.T., D.C. Leard, X. Zhang, P. Davidovits, K.A. Smith, C.E. Kolb, and D.R.Worsnop, Development of an Aerosol Mass Spectrometer for Size and Composition. Analysis of Submicron Particles, Aerosol Science and Technology, 33, 49-70, doi:10.1080/027868200410840, 2000.

Jimenez, J. L., Canagaratna, M. R., Donahue, N. M., Prevot, A. S.H., Zhang, Q., Kroll, J. H., DeCarlo, P. F., Allan, J. D., Coe, H., Ng, N. L., Aiken, A. C., Docherty, K. D., Ulbrich, I. M., Grieshop, A. P., Robinson, A. L., Duplissy, J., Smith, J. D., Wilson, K. R., Lanz, V. A., Hueglin, C., Sun, Y. L., Tian, J., Laaksonen, A., Raatikainen, T., Rautiainen, J., Vaattovaara, P., Ehn, M., Kulmala, M., Tomlinson, J. M., Collins, D. R., Cubison, M. J., Dunlea, E. J., Huffman, J. A., Onasch, T. B., Alfarra, M. R., Williams, P. I., Bower, K., Kondo, Y., Schneider, J., Drewnick, F., Borrmann, S., Weimer, S., Demerjian, K., Salcedo, D., Cottrell, L., Griffin, R., Takami, A., Miyoshi, T., Hatakeyama, S., Shimono, A., Sun, J. Y., Zhang, Y. M., Dzepina, K., Kimmel, J.R., Sueper, D., Jayne, J. T., Herndon, S. C., Trimborn, A. M., Williams, L. R.,Wood, E. C., Kolb, C. E., Baltensperger, U., and Worsnop, D. R.: Evolution of organic aerosol in the atmosphere, Science, 326, 1525–1529, doi:10.1126/science.1180353, 2009.

Kalogridis, A.-C., Vratolis, S., Liakakou, E., Gerasopoulos, E., Mihalopoulos, N., and Eleftheriadis, K.: Assessment of wood burning versus fossil fuel contribution to wintertime black carbon and carbon monoxide concentrations in Athens, Greece, Atmos. Chem. Phys. Discuss., https://doi.org/10.5194/acp-2017-854, in review, 2017.

Kaltsonoudis, C., Kostenidou, E., Louvaris, E., Psichoudaki, M., Tsiligiannis, E., Florou, K., Liangou, A., and Pandis, S. N.: Characterization of fresh and aged organic aerosol emissions

from meat charbroiling, Atmos. Chem. Phys., 17, 7143-7155, doi: 10.5194/acp-17-7143-2017, 2017.

Kassomenos, P., Kotroni, V., and Kallos, G.: Analysis of climatological and air quality observations from Greater Athens Area, Atmos. Environ., 29, 3671-3688, doi:10.1016/1352-2310(94)00358-R, 1995.

Kanakidou, M., Mihalopoulos, N., Kindap, T., Im, U., Vrekoussis, M., Gerasopoulos, E., Dermitzaki, E., Unal, A., Koçak, M., Markakis, K., Melas, D., Kouvarakis, G., Youssef, A.F., Richter, A., Hatzianastassiou, N., Hilboll, A., Ebojie, F., Wittrock, F., Von Savigny, C., Burrows, J.P., Ladstaetter-Weissenmayer, A., Moubasher, H.: Megacities as hot spots of air pollution in the East Mediterranean, Atmos. Environ. 45, 1223-1235, doi: 10.1016/j.atmosenv.2010.11.048, 2011.

Kazadzis, S., Founda, D., Psiloglou, B. E., Kambezidis, H., Mihalopoulos, N., Sanchez-Lorenzo, A., Meleti, C., Raptis, P. I., Pierros, F., and Nabat, P.: Long-term series and trends in surface solar radiation in Athens, Greece, Atmos. Chem. Phys., 18, 2395-2411, doi: 10.5194/acp-18-2395-2018, 2018.

Kostenidou, E., Lee, B.-H., Engelhart, G. J., Pierce, J. R., and Pandis, S. N.: Mass spectra deconvolution of low, medium and high volatility biogenic Secondary Organic Aerosol, Environ. Sci. Technol., 43, 4884–4889, doi:10.1021/es803676g, 2009.

Kostenidou, E., Florou, K., Kaltsonoudis, C., Tsiflikiotou, M., Vratolis, S., Eleftheriadis, K., and Pandis, S. N.: Sources and chemical characterization of organic aerosol during the summer in the eastern Mediterranean, Atmos. Chem. Phys., 15, 11355-11371, doi:10.5194/acp-15-11355-2015, 2015.

Lanz, V. A., Alfarra, M. R., Baltensperger, U., Buchmann, B., Hueglin, C., Szidat, S., Wehrli, M. N., Wacker, L., Weimer, S., Caseiro, A., Puxbaum, H., and Prevot, A. S. H.: Source attribution of submicron organic aerosols during wintertime inversions by advanced factor analysis of aerosol mass spectra, Environ. Sci. Technol., 42 (1), 214–220, doi:10.1021/es0707207, 2008.

Lathem, T. L., Beyersdorf, A. J., Thornhill, K. L., Winstead, E. L., Cubison, M. J., Hecobian, A., Jimenez, J. L., Weber, R. J., Anderson, B. E., and Nenes, A.: Analysis of CCN activity of Arctic aerosol and Canadian biomass burning during summer 2008, Atmos. Chem. Phys., 13, 2735–2756, doi:10.5194/acp-13-2735-2013, 2013.

Mariani, R.L. and de Mello, W.Z.: $PM_{2.5-10}$, $PM_{2.5}$ and associated water-soluble inorganic species at a coastal urban site in the metropolitan region of Rio de Janeiro, Atmos. Environ., 41, 2887-2892, doi:10.1016/j.atmosenv.2006.12.009, 2007.

Markou, M.T., Kassomenos, P.: Cluster analysis of five years of back trajectories arriving in Athens, Greece, Atmos. Res., 98, 438-457, doi:10.1016/j.atmosres.2010.08.006, 2010.

Ng, N. L., Herndon, S. C., Trimborn, A., Canagaratna, M. R., Croteau, P. L., Onasch, T. B., Sueper, D.,Worsnop, D. R., Zhang, Q., Sun, Y. L., and Jayne, J. T.: An Aerosol Chemical Speciation Monitor (ACSM) for routine monitoring of the composition and mass concentration of ambient aerosol, Aerosol Sci. Technol., 45, 780–794, doi:10.1080/02786826.2011.560211, 2011a.

Ng, N. L., Canagaratna, M. R., Jimenez, J. L., Zhang, Q., Ulbrich, I. M., and Worsnop, D. R.: Real-time methods for estimating organic component mass concentrations from aerosol mass spectrometer data, Environ. Sci. Technol., 45, 910–916, doi:10.1021/es102951k, 2011b.

Orsini, D.A., Ma, Y., Sullivan, A., Sierau, B., Baumann, K., Weber, R.J.: Refinements to the particle-into-liquid sampler (PILS) for ground and airborne measurements of water soluble aerosol composition, Atmos. Environ. 37 (9-10), 1243-1259, doi:10.1016/S1352-2310(02)01015-4, 2003.

Paatero, P. and Hopke, P.K.: Discarding or downweighting high-noise variables in factor analytic models, Analytica Chimica Acta, 490(1-2), 277-289, doi:10.1016/S0003-2670(02)01643-4, 2003.

Paatero, P. and Tapper, U.: Positive matrix factorization: A non-negative factor model with optimal utilization of error estimates of data values. Environmetrics, 5(2), 111-126, doi:10.1002/env.3170050203, 1994.

Paraskevopoulou, D., Liakakou, E., Gerasopoulos, E., Theodosi, C., Mihalopoulos, N.: Long-term characterization of organic and elemental carbon in the PM2.5 fraction: the case of Athens Greece, Atmos. Chem. Phys. 14, 13313-13325, doi:10.5194/acp-14-13313-2014, 2014.

Paraskevopoulou, D, Liakakou, E., Gerasopoulos, E., and Mihalopoulos, N.: Sources of atmospheric aerosol from long-term measurements (5years) of chemical composition in Athens, Greece, Sci. Tot. Environ., 527-528, 165-178, doi:10.1016/j.scitotenv.2015.04.022, 2015.

Park, S.S., Ondov, J.M., Harrison, D., and Nair, N.P.: Seasonal and short-term variations in particulate atmospheric nitrate in Baltimore, Atmos. Environ., 39, 2011-2020, doi:10.1016/j.atmosenv.2004.12.032, 2005.

Paschalidou, A.K., Kassomenos, P., Karanikola, P.: Disaggregating the contribution of local dispersion and long-range transport to the high PM_{10} values measured in a Mediterranean urban environment, Sci. Total Environ., 527-528, 119-125, doi: 10.1016/j.scitotenv.2015.04.094, 2015.

Pateraki, St, Asimakopoulos, D.N., Bougiatioti, A., Maggos, Th, Vasilakos, Ch, and Mihalopoulos, N.: Assessment of PM2.5 and PM1 chemical profile in a multiple-impacted Mediterranean urban area: origin, sources and meteorological dependence, Sci. Total Environ. 479, 210-220, doi:10.1016/j.scitotenv.2014.02.008, 2014.

Petit, J.-E., Favez, O., Sciare, J., Crenn, V., Sarda-Estève, R., Bonnaire, N., Močnik, G., Dupont, J.-C., Haeffelin, M., and Leoz-Garziandia, E.: Two years of near real-time chemical composition of submicron aerosols in the region of Paris using an Aerosol Chemical Speciation Monitor (ACSM) and a multi-wavelength Aethalometer, Atmos. Chem. Phys., 15, 2985-3005, doi: 10.5194/acp-15-2985-2015, 2015.

Puxbaum, H., Caseiro, A., Sanchez-Ochoa, A., Kasper-Giebl, A., Claeys, M., Gerencser, A., Legrand, M., Preunkert, S., and Pio, C.A.: Levoglucosan levels at background sites in Europe for assessing the impact of biomass combustion on the European aerosol background, J. Geophys. Res. Atmos. 112 (23), D23S05, doi:10.1029/2006JD008114, 2007.

Saarikoski, S., Carbone, S., Decesari, S., Giulianelli, L., Angelini, F., Canagaratna, M., Ng, N. L., Trimborn, A., Facchini, M. C., Fuzzi, S., Hillamo, R., and Worsnop, D.: Chemical characterization of springtime submicrometer aerosol in Po Valley, Italy, Atmos. Chem. Phys., 12, 8401-8421, doi:10.5194/acp-12-8401-2012, 2012.

Saffari, A., Daher, N., Samara, C., Voutsa, D., Kouras, A., Manoli, E., Karagkiozidou, O., Vlachokostas, C., Moussiopoulos, N., Shafer, M.M., Schauer, J.J., and Sioutas, C.: Increased Biomass Burning Due to the Economic Crisis in Greece and Its Adverse Impact on Wintertime Air Quality in Thessaloniki. Environmental Science & Technology, 47 (23), 13313, doi:10.1021/es403847h, 2013.

Sage, A. M., Weitkamp, E. A., Robinson, A. L., and Donahue, N. M.: Evolving mass spectra of the oxidized component of organic aerosol: results from aerosol mass spectrometer analyses

of aged diesel emissions, Atmos. Chem. Phys., 8, 1139-1152, doi:10.5194/acp-8-1139-2008, 2008.

Sandradewi, J., Prevot, A. S. H., Szidat, S., Perron, N., Lanz, V. A., Weingartner, E., and Baltensperger, U.: Using aerosol light absorption measurements for the quantitative determination of wood burning and traffic emission contributions to particulate matter, Environ. Sci. Technol., 42, 3316–3323, doi:10.1021/es702253m, 2008.

Santos, F. C., Longo, K. M., Guenther, A. B., Kim, S., Gu, D., Oram, D. E., Forster, G. L., Lee, J., Hopkins, J. R., Brito, J. F., and Freitas, S. R.: Biomass burning emissions disturbances on the isoprene oxidation in a tropical forest, Atmos. Chem. Phys. Discuss., doi:10.5194/acp-2017-1083, in review, 2017.

Schneider, J., Weimer, S., Drewnick, F., Borrmann, S., Helas, G., Gwaze, P., Schmid, O., Andreae, M.O. and Kirchner, U.: Mass spectrometric analysis and aerodynamic properties of various types of combustion-related aerosol particles, Int. J. Mass Spectrom., 258, 37–49, doi:10.1016/j.ijms.2006.07.008, 2006.

Seinfeld, J.H. and Pandis, S.N., 2016. Atmospheric chemistry and physics: from air pollution to climate change. John Wiley & Sons, 2016.

Sirois, A., Bottenheim, J.W.: Use of backward trajectories to interpret the 5-year record of PAN and O3 ambient air concentrations at Kejimkujik National Park, Nova Scotia, J. Geophys. Res., 100, 2867-2881, doi:10.1029/94JD02951, 1995.

Tombrou, M., Dandou, A., Helmis, C., Akylas, E., Angelopoulos, G., Flocas, H., Assimakopoulos, V. and Soulakellis, N.: Model evaluation of the atmospheric boundary layer and mixed-layer evolution, Boundary-layer meteorology, *124*(1), 61-79, doi:10.1007/s10546-006-9146-5, 2007.

Theodosi, C., Grivas, G., Zarmpas, P., Chaloulakou, A., and Mihalopoulos, N.: Mass and chemical composition of size-segregated aerosols (PM1, PM2.5, PM10) over Athens, Greece: local versus regional sources, Atmos. Chem. Phys., 11, 11895-11911, doi:10.5194/acp-11-11895-2011, 2011.

Ulbrich, I. M., Canagaratna, M. R., Zhang, Q., Worsnop, D. R., and Jimenez, J. L.: Interpretation of organic components from Positive Matrix Factorization of aerosol mass spectrometric data, Atmos. Chem. Phys., 9, 2891-2918, doi:10.5194/acp-9-2891-2009, 2009.

Vrekoussis, M., Richter, A., Hilboll, Al, Burrows, J.P., Gerasopoulos, E., Lelieveld, J., Barrie, L., Zerefos, C., and Mihalopoulos, N.: Economic crisis detected from space: air quality observations over Athens/Greece, Geophys. Res. Let. 40, 458-463, doi:10.1002/grl.50118, 2013.

Wang, Y.Q., Zhang, X.Y., Draxler, R.: TrajStat: GIS-based software that uses various trajectory statistical analysis methods to identify potential sources from long-term air pollution measurement data, Environ. Mod. Softw., 24, 938–939, doi:10.1016/j.envsoft.2009.01.004, 2009.

Atmos. Chem. Phys. Discuss., https://doi.org/10.5194/acp-2018-356
Manuscript under review for journal Atmos. Chem. Phys.
Discussion started: 16 May 2018

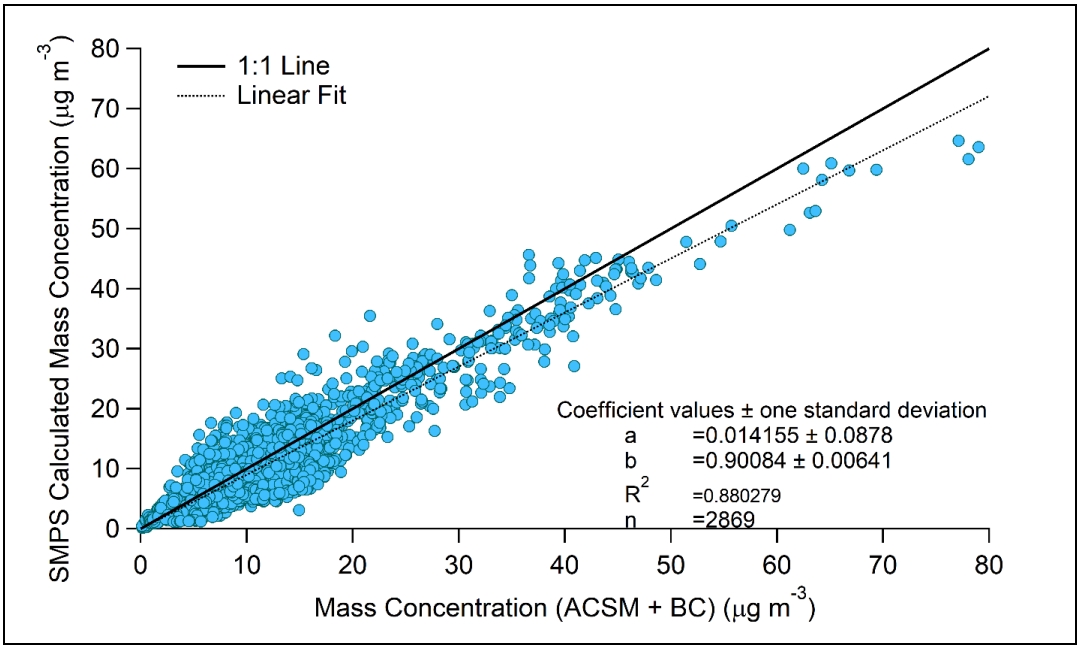

Figure 1: Correlation between ACSM+BC vs. SMPS-derived mass concentrations for the 2016-17 measurement period.

Atmos. Chem. Phys. Discuss., https://doi.org/10.5194/acp-2018-356
Manuscript under review for journal Atmos. Chem. Phys.
Discussion started: 16 May 2018

Atmospheric Chemistry and Physics Discussions

840

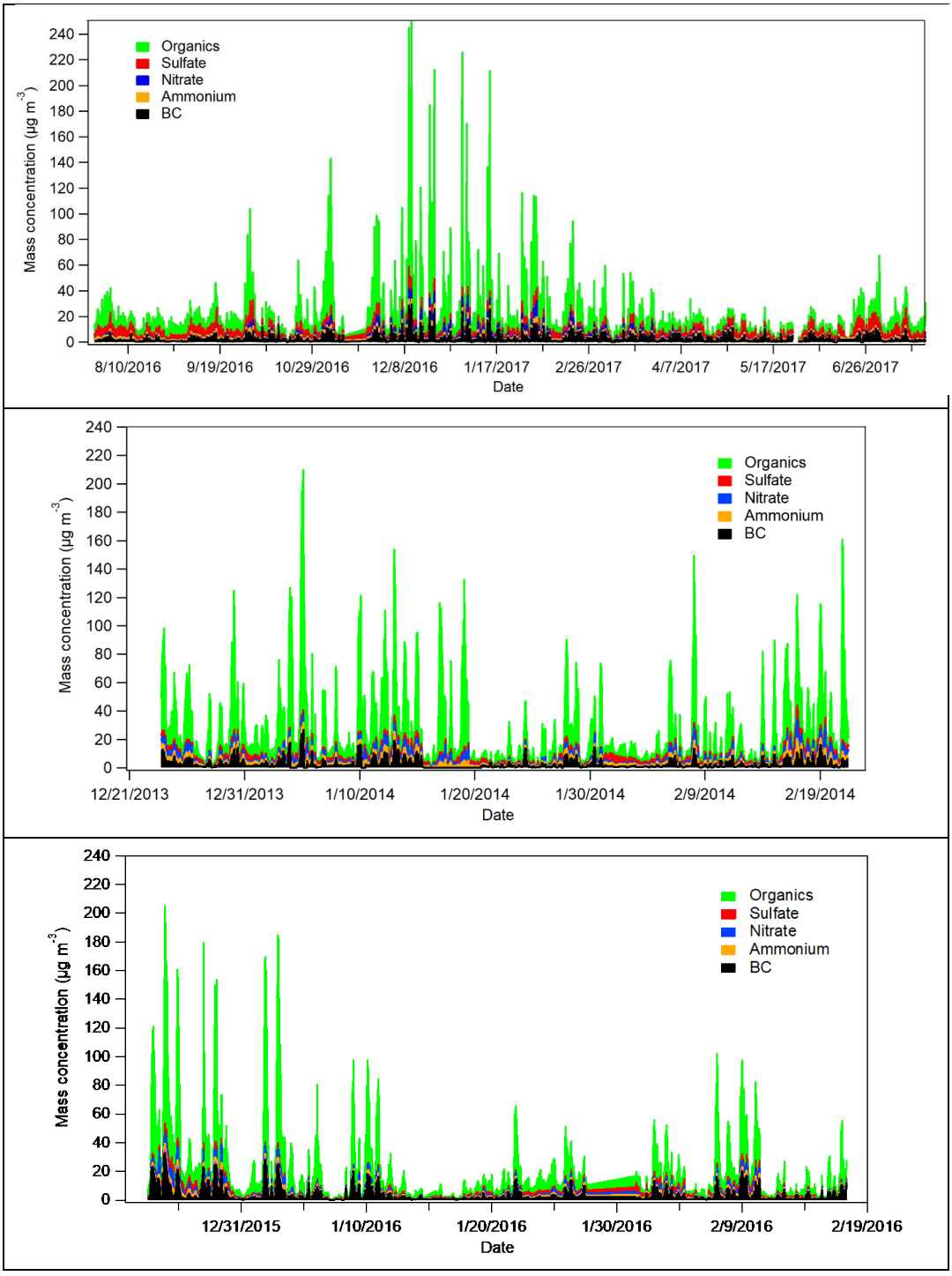

Atmos. Chem. Phys. Discuss., https://doi.org/10.5194/acp-2018-356
Manuscript under review for journal Atmos. Chem. Phys.
Discussion started: 16 May 2018

Figure 2: Time series of the main submicron aerosol components. On the top panel the one-year period starting on 26 July 2016 and ending on 31 July 2017, on the middle panel the 2013-2014 winter campaign (18 December-21 February), and on the bottom panel, the 2015-2016 winter campaign (23 December-17 February).

845

Atmos. Chem. Phys. Discuss., https://doi.org/10.5194/acp-2018-356
Manuscript under review for journal Atmos. Chem. Phys.
Discussion started: 16 May 2018

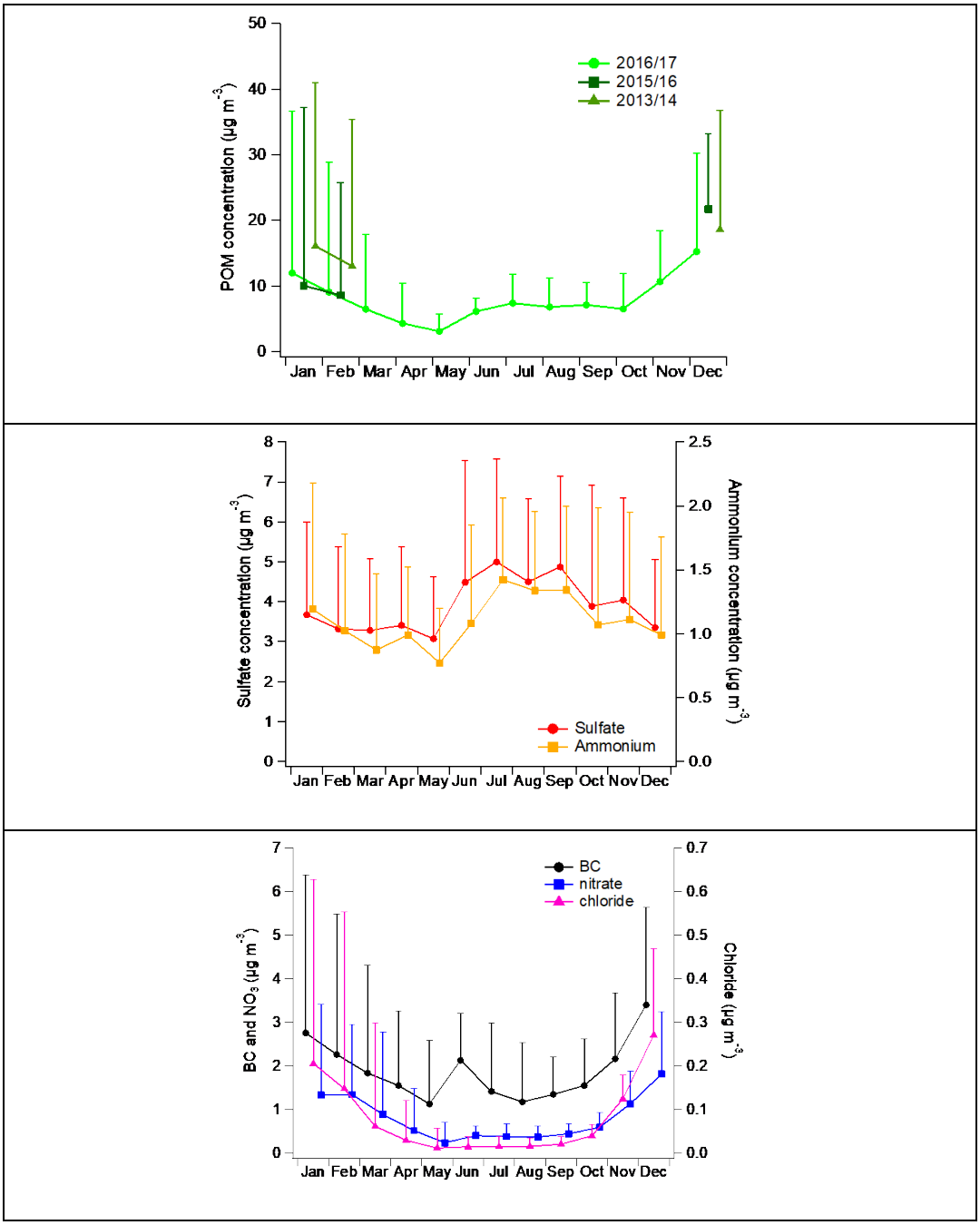

Figure 3: Monthly average concentrations of the main aerosol constituents. Organics are shown on the top panel for the one year 2016-2017 period as well as the 2013-2014 and 2015-2016 winter periods, while sulfate and ammonium on the middle panel, and BC, nitrate and chloride on the bottom panel

shown for the one year 2016-2017 period. Standard deviation is also depicted (error bars; only the positive part is shown for plot's clarity issues).

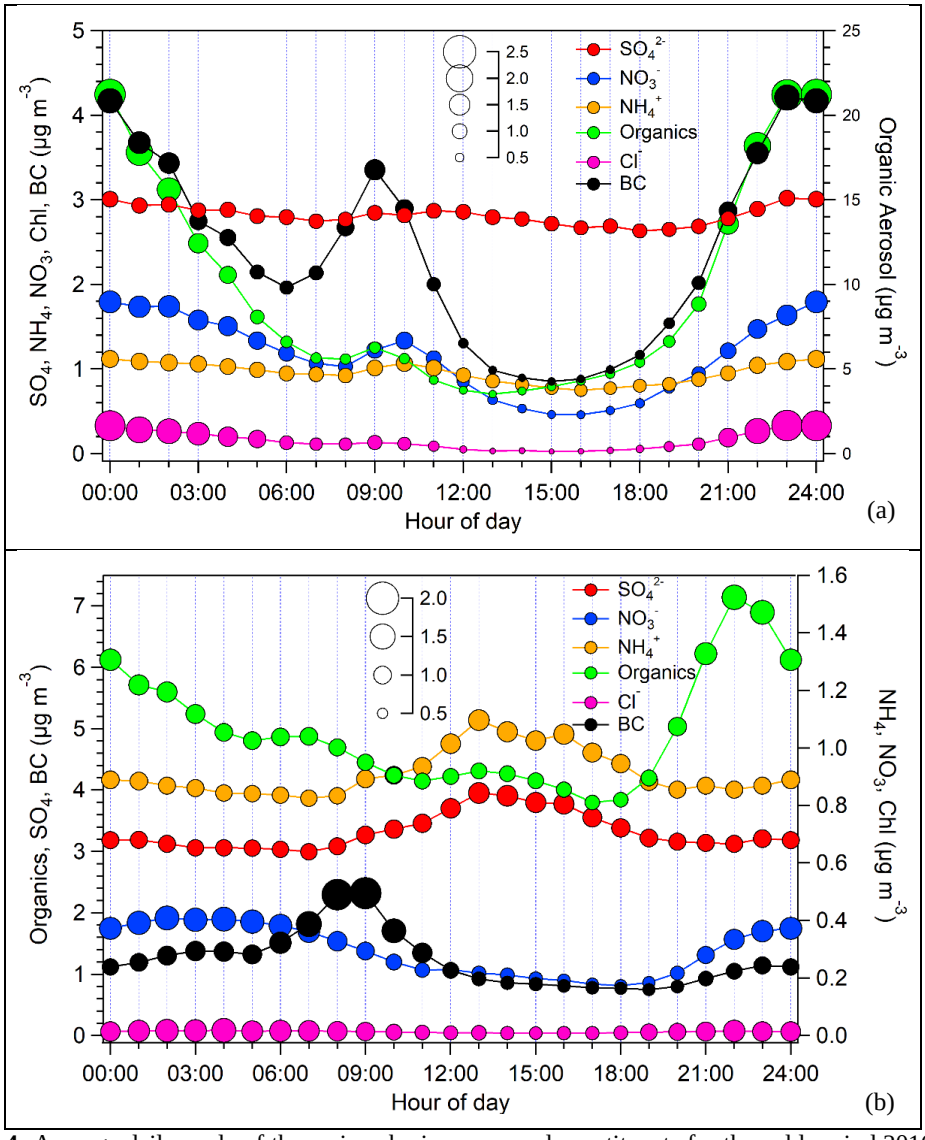

Figure 4: Average daily cycle of the main submicron aerosol constituents for the cold period 2016-17 on the top panel and the warm period of 2017 on the bottom panel. The size of the markers indicates the normalized values relative to each species' daily mean value.

Atmos. Chem. Phys. Discuss., https://doi.org/10.5194/acp-2018-356
Manuscript under review for journal Atmos. Chem. Phys.
Discussion started: 16 May 2018

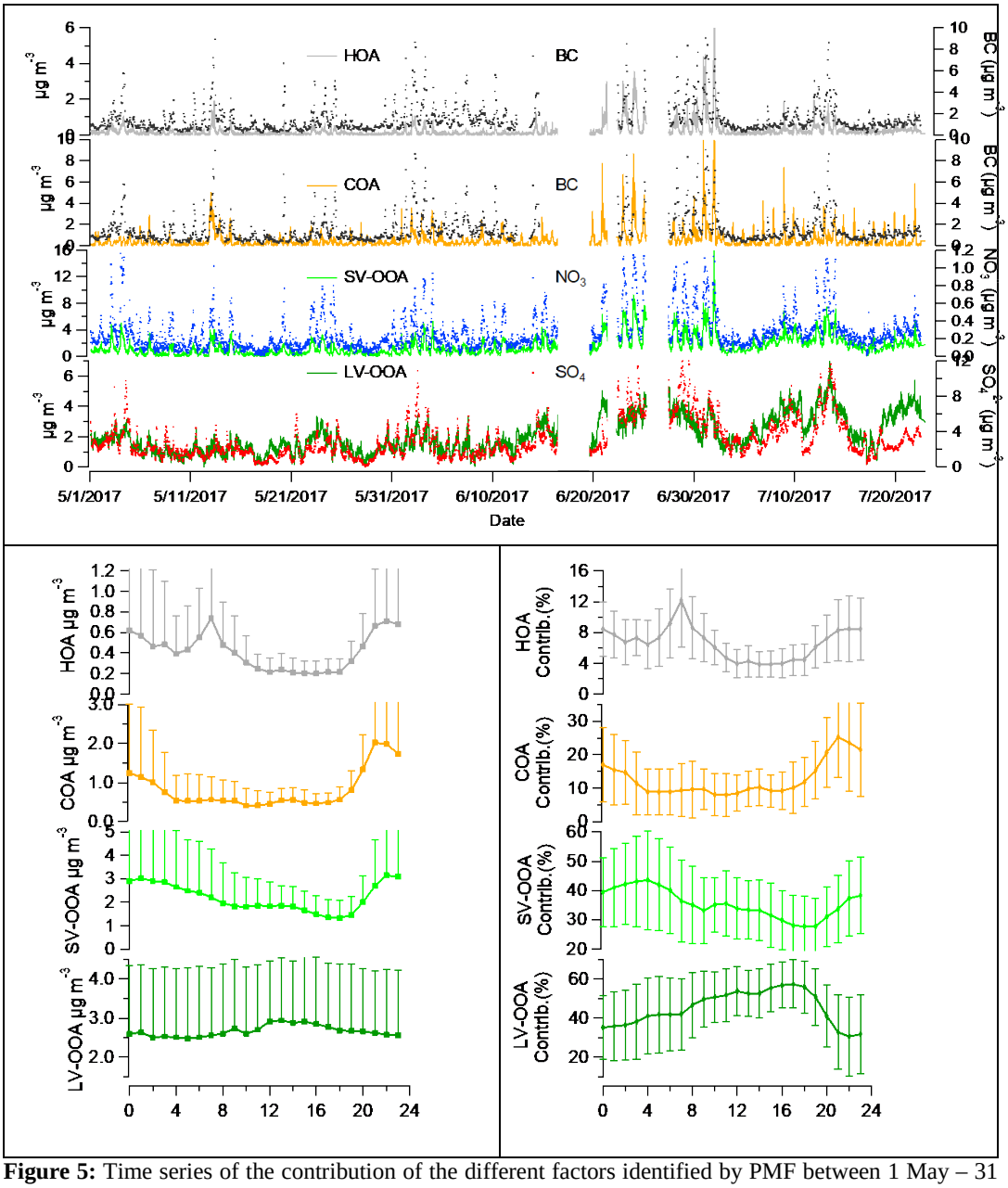

Figure 5: Time series of the contribution of the different factors identified by PMF between 1 May – 31 July 2017 (top) along with their average diurnal cycles (bottom left) and the respective hourly average contributions (bottom right).

860

Atmos. Chem. Phys. Discuss., https://doi.org/10.5194/acp-2018-356
Manuscript under review for journal Atmos. Chem. Phys.
Discussion started: 16 May 2018

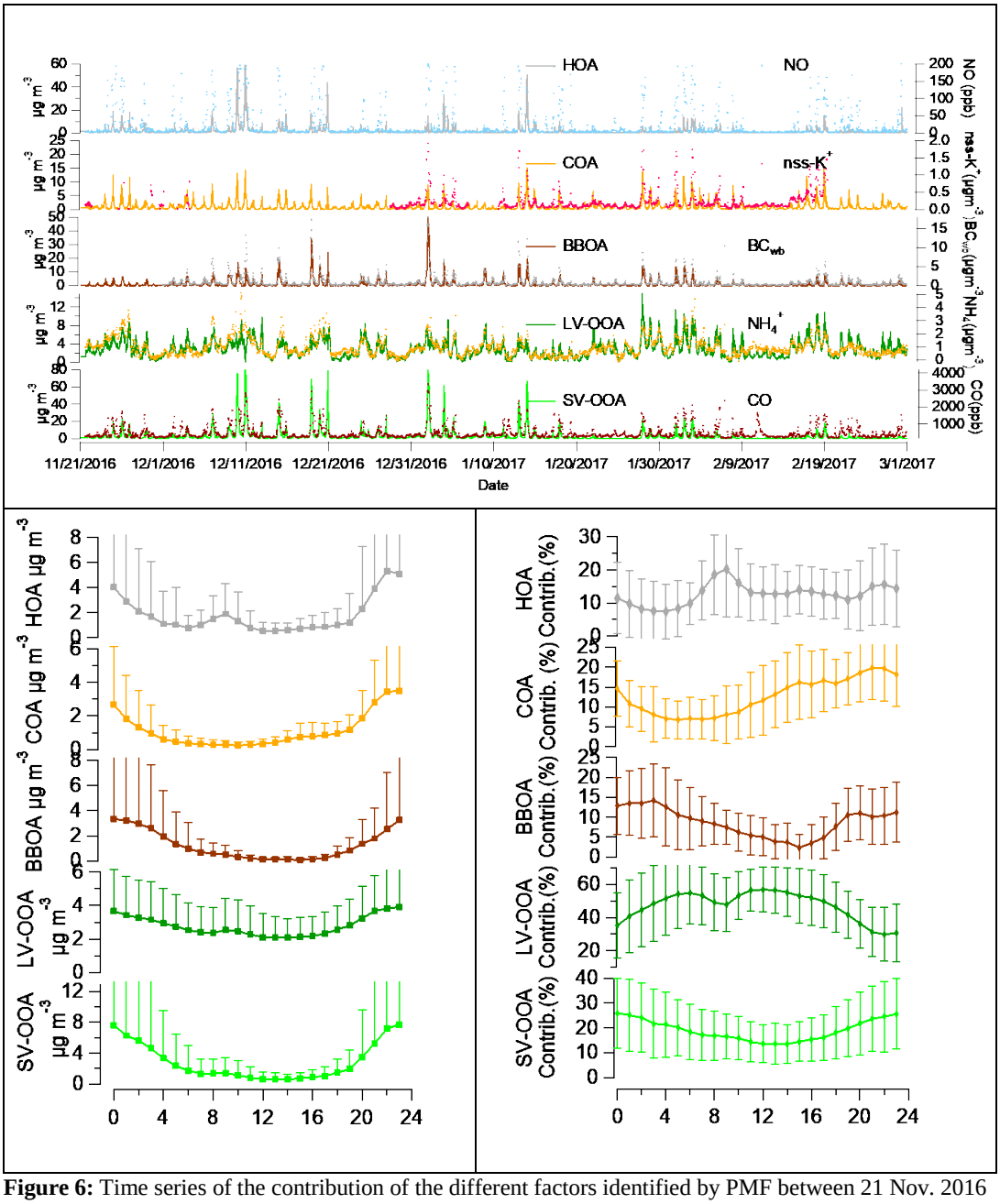

Figure 6: Time series of the contribution of the different factors identified by PMF between 21 Nov. 2016 – 1 March 2017 (top) along with their average diurnal cycle (bottom left) and respective hourly contribution (bottom right).

Atmos. Chem. Phys. Discuss., https://doi.org/10.5194/acp-2018-356
Manuscript under review for journal Atmos. Chem. Phys.
Discussion started: 16 May 2018

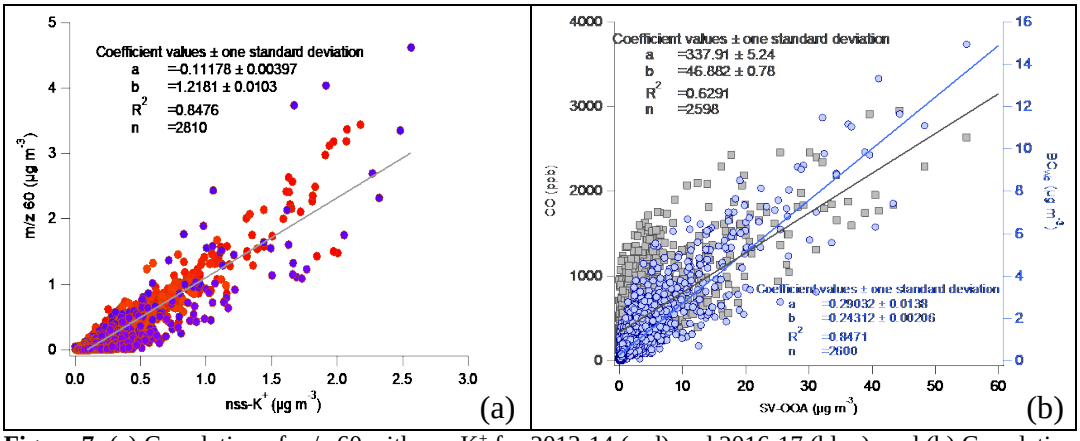

865 **Figure 7:** (a) Correlation of m/z 60 with nss-K^+ for 2013-14 (red) and 2016-17 (blue), and (b) Correlation of SV-OOA with CO (grey) and BC (blue) for 2016-17.

Atmos. Chem. Phys. Discuss., https://doi.org/10.5194/acp-2018-356
Manuscript under review for journal Atmos. Chem. Phys.
Discussion started: 16 May 2018

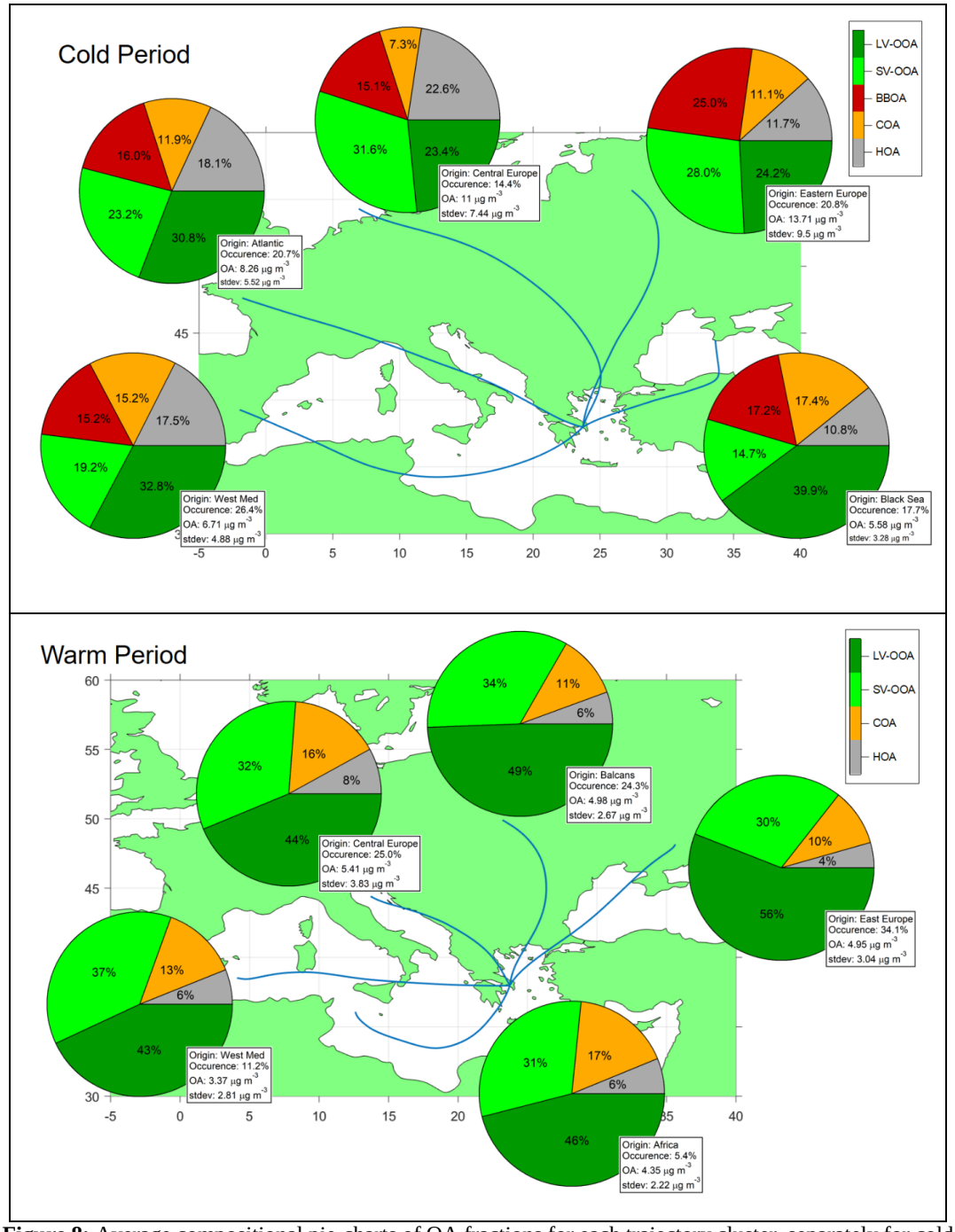

Figure 8: Average compositional pie-charts of OA fractions for each trajectory cluster, separately for cold (November 2016 – March 2017) and warm (Aug-Sep 2016 and May-Jul 2017) periods on the top and

870 bottom panel respectively. Displaying also frequency of occurrence and average OA concentrations for each cluster.

	MAM 2017	**JA 2016& JJ 2017**	**SON 2016**	**DJF 2016-17**	**DJF 2013-14**	**DJF 2015-16**
Organics	3.5 ± 3.3 (0.3-35.9)	5.3 ± 3.4 (0.4-44.8)	6.3 ± 7.9 (0.3-98.6)	9.9 ± 16.1 (0.2-200.5)	15.7 ± 21.8 (0.5-189.4)	11.5 ± 18.4 (0.7-151.4)
Ammonium	0.6 ± 0.5 (0.4-2.9)	1.0 ± 0.6 (0.2-3.9)	1.1 ± 0.7 (0.4-5.1)	1.0 ± 0.7 (0.2-5.1)	1.9 ± 1.3 (0.2-9.9)	1.0 ± 0.9 (0.3-6.2)
Sulfate	2.8 ± 1.4 (0.2-9.7)	3.6 ± 2.0 (0.2-14.5)	3.5 ± 2.2 (0.2-15.4)	2.7 ± 1.7 (0.2-14.8)	2.3 ± 1.3 (0.3-12.3)	2.2 ± 1.5 (0.4-9.3)
Nitrate	0.4 ± 0.5 (0.05-4.8	0.3 ± 0.2 (0-1.4)	0.6 ± 0.8 (0.1-6.5)	1.2 ± 1.5 (0.05-11.1)	2.1 ± 2.0 (0.09-15.4)	1.4 ± 1.8 (0.07-9.9)
Chloride	0.03 ± 0.05 (0-0.9)	0.02 ± 0.02 (0.04-0.2)	0.05 ± 0.1 (0.08-2.0)	0.17 ± 0.33 (0-3.7)	0.14 ± 0.22 (0.08-6.8)	0.11 ± 0.24 (0-2.5)
BC	1.5 ± 1.4 (0.1-14.6)	1.2 ± 0.8 (0.2-10.5)	1.7 ± 1.6 (0.1-12.4)	2.4 ± 3.4 (0.1-29.6)	2.7 ± 3.2 (0.2-26.8)	3.4 ± 4.6 (0.2-32.3)
PM1	10.2 ± 7.1 (0.6-115.6)	9.6 ± 6.2 (0.5-67.4)	15.8 ± 13.2 (0.9-143.9)	20.7 ± 26.4 (0.8-251.8)	25.1 ± 29.9 (1.4-213.1)	19.5 ± 25.3 (1.7-202.5)

Table 1: Seasonal average concentrations ± standard deviation (range) and total mass of the main submicron aerosol components for the one-year study period and the two winter campaigns.

875

Atmos. Chem. Phys. Discuss., https://doi.org/10.5194/acp-2018-356
Manuscript under review for journal Atmos. Chem. Phys.
Discussion started: 16 May 2018

Atmospheric Chemistry and Physics Discussions

	Winter 2013-14 18/12/13 – 21/02/14	**Winter 2015-16** 23/12/15 – 17/02/16	Cold **2016-17** 01/11/16-18/03/17
BBOA	8.3%	9%	10.3%
HOA	16%	12.5%	16.5%
COA	7.4%	7.2%	11.4%
SV-OOA	33.1%	27.5%	30.8%
LV-OOA	35.2%	43.8%	31%

Table 2: Contribution of the five organic aerosol components to the total organic fraction during the three individual winter campaigns.